

Critical Mineral Resources of the United States— Economic and Environmental Geology and Prospects for Future Supply




Professional Paper 1802

**U.S. Department of the Interior
U.S. Geological Survey**


Periodic Table of Elements

1A																	8A				
1 H hydrogen 1.008																	2 He helium 4.003				
3 Li lithium 6.94	4 Be beryllium 9.012															5 B boron 10.81	6 C carbon 12.01	7 N nitrogen 14.01	8 O oxygen 16.00	9 F fluorine 19.00	10 Ne neon 20.18
11 Na sodium 22.99	12 Mg magnesium 24.31															13 Al aluminum 26.98	14 Si silicon 28.09	15 P phosphorus 30.97	16 S sulfur 32.06	17 Cl chlorine 35.45	18 Ar argon 39.95
19 K potassium 39.10	20 Ca calcium 40.08	21 Sc scandium 44.96	22 Ti titanium 47.88	23 V vanadium 50.94	24 Cr chromium 52.00	25 Mn manganese 54.94	26 Fe iron 55.85	27 Co cobalt 58.93	28 Ni nickel 58.69	29 Cu copper 63.55	30 Zn zinc 65.39	31 Ga gallium 69.72	32 Ge germanium 72.64	33 As arsenic 74.92	34 Se selenium 78.96	35 Br bromine 79.90	36 Kr krypton 83.79				
37 Rb rubidium 85.47	38 Sr strontium 87.62	39 Y yttrium 88.91	40 Zr zirconium 91.22	41 Nb niobium 92.91	42 Mo molybdenum 95.96	43 Tc technetium (98)	44 Ru ruthenium 101.1	45 Rh rhodium 102.9	46 Pd palladium 106.4	47 Ag silver 107.9	48 Cd cadmium 112.4	49 In indium 114.8	50 Sn tin 118.7	51 Sb antimony 121.8	52 Te tellurium 127.6	53 I iodine 126.9	54 Xe xenon 131.3				
55 Cs cesium 132.9	56 Ba barium 137.3	*	72 Hf hafnium 178.5	73 Ta tantalum 180.9	74 W tungsten 183.9	75 Re rhenium 186.2	76 Os osmium 190.2	77 Ir iridium 192.2	78 Pt platinum 195.1	79 Au gold 197.0	80 Hg mercury 200.5	81 Tl thallium 204.4	82 Pb lead 207.2	83 Bi bismuth 209.0	84 Po polonium (209)	85 At astatine (210)	86 Rn radon (222)				
87 Fr francium (223)	88 Ra radium (226)	**	104 Rf rutherfordium (261)	105 Db dubnium (268)	106 Sg seaborgium (271)	107 Bh bohrium (270)	108 Hs hassium (277)	109 Mt meitnerium (276)	110 Ds darmstadtium (281)	111 Rg roentgenium (280)	112 Cn copernicium (285)	113 Uut (284)	114 Fl flerovium (289)	115 Uup (288)	116 Lv livermorium (293)	117 Uus (294)	118 Uuo (294)				
Lanthanide Series*		57 La lanthanum 138.9	58 Ce cerium 140.1	59 Pr praseodymium 140.9	60 Nd neodymium 144.2	61 Pm promethium (145)	62 Sm samarium 150.4	63 Eu europium 152.0	64 Gd gadolinium 157.2	65 Tb terbium 158.9	66 Dy dysprosium 162.5	67 Ho holmium 164.9	68 Er erbium 167.3	69 Tm thulium 168.9	70 Yb ytterbium 173.0	71 Lu lutetium 175.0					
Actinide Series**		89 Ac actinium (227)	90 Th thorium 232	91 Pa protactinium 231	92 U uranium 238	93 Np neptunium (237)	94 Pu plutonium (244)	95 Am americium (243)	96 Cm curium (247)	97 Bk berkelium (247)	98 Cf californium (251)	99 Es einsteinium (252)	100 Fm fermium (257)	101 Md mendelevium (288)	102 No nobelium (259)	103 Lr lawrencium (262)					



Los Alamos

NATIONAL LABORATORY



element names in **blue** are liquids at room temperature

element names in **red** are gases at room temperature

element names in **black** are solids at room temperature

Modified from Los Alamos National Laboratory Chemistry Division; available at <http://periodic.lanl.gov/images/periodictable.pdf>.

Front cover (clockwise starting at top left).

Dry Lake Wind Power Project. This 63-megawatt-capacity facility in Arizona was the first utility-scale power project. The large wind turbines use generators that contain strong permanent magnets composed of neodymium-iron-boron. Photograph courtesy of Iberdrola Renewables, Inc., NREL 16701.

U.S. Air Force F-35 Lightning II Joint Strike Fighter. This and many other aerospace vehicles rely on electrical and mechanical components made of beryllium alloys. Photograph courtesy of the U.S. Air Force.

Flat-panel display and touchscreen devices. The screens are coated with indium-tin oxide, for which there are few chemical substitutes. Photograph by C.N. Mercer, U.S. Geological Survey.

Solar photovoltaic cells. This 2-megawatt ground-mounted array occupies the site of a former landfill at Fort Carson, Colorado. Tellurium is a critical component for the development of efficient thin-film photovoltaic cells that are needed for the production of electricity from sunlight. Photograph courtesy of the U.S. Department of Energy Western Area Power Administration.

Back cover. A handful of stibnite, which is the primary ore mineral for antimony. Antimony is widely used in plastics, rubbers, paints, and textiles, including industrial safety suits and some children's clothing, to make them resistant to the spread of flames. Photograph by Niki Wintzer, U.S. Geological Survey.

Front and back covers background image. Lithium-brine evaporating ponds at Clayton Valley, Nevada. Lithium has many uses, the most prominent being in batteries for cell phones, laptop computers, and electric and hybrid vehicles. Photograph by Doc Searls/CC-BY-2.0, http://commons.wikimedia.org/wiki/File:Chemetall_Foote_Lithium_Operation.jpg.

Critical Mineral Resources of the United States—Economic and Environmental Geology and Prospects for Future Supply

Edited by Klaus J. Schulz, John H. DeYoung, Jr., Robert R. Seal II
and Dwight C. Bradley

Professional Paper 1802

**U.S. Department of the Interior
U.S. Geological Survey**

U.S. Department of the Interior
SALLY JEWELL, Secretary

U.S. Geological Survey
Suzette M. Kimball, Director

U.S. Geological Survey, Reston, Virginia: 2017

For more information on the USGS—the Federal source for science about the Earth, its natural and living resources, natural hazards, and the environment—visit <http://www.usgs.gov> or call 1–888–ASK–USGS.

For an overview of USGS information products, including maps, imagery, and publications, visit <http://store.usgs.gov/>.

Any use of trade, firm, or product names is for descriptive purposes only and does not imply endorsement by the U.S. Government.

Although this information product, for the most part, is in the public domain, it also may contain copyrighted materials as noted in the text. Permission to reproduce copyrighted items must be secured from the copyright owner.

Suggested citation:

Schulz, K.J., DeYoung, J.H., Jr., Seal, R.R., II, and Bradley, D.C., eds., 2017, Critical mineral resources of the United States—Economic and environmental geology and prospects for future supply: U.S. Geological Survey Professional Paper 1802, 798 p., <http://dx.doi.org/10.3133/pp1802>.

Library of Congress Cataloging-in-Publication Data

Names: Schulz, K. J., editor. | Geological Survey (U.S.), issuing body.
Title: Critical mineral resources of the United States : economic and environmental geology and prospects for future supply / edited by Klaus J. Schulz, John H. DeYoung, Jr., Robert R. Seal II, and Dwight C. Bradley.
Other titles: Economic and environmental geology and prospects for future supply | U.S. Geological Survey professional paper ; 1802.
Description: Reston, Virginia : U.S. Geological Survey, [2017] | Series: Professional paper ; 1802 | Includes bibliographical references.
Identifiers: LCCN 2017005489 | ISBN 9781411339910 | ISBN 1411339916
Subjects: LCSH: Mines and mineral resources--United States. | Strategic materials--United States. | Industrial minerals--United States.
Classification: LCC TN23 .C67 2017 | DDC 333.8/50973--dc23 | SUDOC I 19.16:1802
LC record available at <https://lcn.loc.gov/2017005489>

ISSN 1044-9612 (print)
ISSN 2330-7102 (online)

Foreword

From the Stone, Bronze, and Iron Ages, through the Industrial Revolution, to the emergence of developing nations and economies in the 21st century, mineral commodities have been essential ingredients for building and advancing civilization. Our homes and office buildings, our cars and the roads we drive on, and our computers, televisions, and smart phones are but a few examples of things we use every day that are built with materials derived from mineral resources. In short, minerals are important to a modern society.

When the periodic table of elements was first established in the latter half of the 19th century, many of the elements were simply known to exist in nature, but, compared to today, relatively few were being used by society. Today, the discovery of new uses for an increasing number of elements on the periodic table is enabling rapid innovations in technology and materials science. Advances in telecommunications, information technology, health care, alternative energy technology, and national defense systems have all been made possible through the incorporation of new mineral materials.

As the importance and dependence on use of specific mineral commodities grow, so does the concern about their supply. Mineral commodities that have important uses and no viable substitutes, yet face potential disruption in supply, are defined as critical to the Nation's economic and national security. A mineral commodity's importance and the nature of its supply chain can change with time, such that a mineral commodity that may have been considered critical 25 years ago may not be critical now, and one considered critical now may not be so in the future.

The U.S. Geological Survey has produced this volume to describe a select group of important mineral commodities of our time and to document where the United States stands in the changing spectrum of mineral commodity needs and availability. For each mineral commodity covered, the authors provide a comprehensive look at the commodity's use, the geology and global distribution of the mineral deposit types that account for the present and possible future supply of the commodity, and the current status of production, reserves and resources, both in the United States and globally. Information is also provided on mineral environmental issues to be considered in the responsible development of different types of mineral deposits. This analysis describes U.S. critical mineral resources in a global context, for no country can be self-sufficient for all its mineral commodity needs, and the United States will always rely on global mineral commodity supply chains. This volume provides the scientific understanding of critical mineral resources that is required for informed decisionmaking by those responsible for ensuring that the United States has a secure and sustainable supply of the mineral commodities that it needs. For just as our past was built on a foundation of minerals, even more so will be our future.

A handwritten signature in black ink, reading "Sally Jewell". The signature is fluid and cursive, with the first name "Sally" and last name "Jewell" clearly distinguishable.

Sally Jewell
Secretary of the Interior

Preface

Mineral commodities are vital to economic growth, improving the quality of life, providing for national defense, and the overall functioning of modern society. Minerals are being used in larger quantities than ever before and in an increasingly diverse range of applications from telecommunications (cell phones and computers) to renewable-energy generation (wind turbines, solar photovoltaics, and fuel cells) to clean forms of transportation (electric and hybrid cars). Until the mid-20th century, only about 15 metallic elements had much practical use. Today, nearly all the natural elements in the periodic table of elements have several significant uses. For example, the manufacture of a modern computer chip requires more than one-half of the elements in the periodic table. Even though many of the elements may be present in only small amounts, each is essential to the function and performance of the chip.

With the increasing demand for a considerably more diverse suite of mineral commodities has come renewed recognition that competition and conflict over mineral resources can pose significant risks to the manufacturing industries that depend on them. In addition, although mineral deposits may occur in many places around the world, production of many mineral commodities today has become concentrated in relatively few countries (for example, tungsten, rare-earth elements, and antimony in China; niobium in Brazil; and platinum-group elements in South Africa and Russia), thus increasing the risk for supply disruption owing to political, social, or other factors. At the same time, an increasing awareness and sensitivity to potential environmental and health issues caused by the mining and processing of many mineral commodities may place additional restrictions on mineral supplies. These factors have led a number of Governments, including the Government of the United States, to attempt to identify those mineral commodities that are viewed as most “critical” to the national economy and (or) security if supplies should be curtailed. The lists of critical minerals compiled by Governments and other organizations vary in the number and individual rankings of mineral commodities included on them, but many of the lists include several of the same commodities. Rare-earth elements and platinum-group elements particularly are broadly viewed as critical.

This book presents resource and geologic information on the following 23 mineral commodities currently among those viewed as important to the national economy and national security of the United States: antimony (Sb), barite (barium, Ba), beryllium (Be), cobalt (Co), fluorite or fluorspar (fluorine, F), gallium (Ga), germanium (Ge), graphite (carbon, C), hafnium (Hf), indium (In), lithium (Li), manganese (Mn), niobium (Nb), platinum-group elements (PGE), rare-earth elements (REE), rhenium (Re), selenium (Se), tantalum (Ta), tellurium (Te), tin (Sn), titanium (Ti), vanadium (V), and zirconium (Zr). For a number of these commodities—for example, graphite, manganese, niobium, and tantalum—the United States is currently wholly dependent on imports to meet its needs.

The first two chapters deal with general information pertinent to the study of mineral resources. The introductory chapter (A) discusses the purposes of the volume, the distinctions between reserves and various categories of resources, and issues related to the classification of mineral resource “criticality.” The second chapter (B) provides an overview of some of the environmental considerations related to the mining of nonfuel mineral resources, including the modern regulatory framework and development of geoenvironmental mineral-deposit models.

Chapters C through V describe individual mineral commodities and include an overview of current uses of the commodity, identified resources and their distribution nationally and globally, the state of current geologic knowledge, the potential for finding additional deposits nationally and globally, and geoenvironmental issues that may be related to the production and uses of the commodity. These chapters are updates of the commodity chapters published in 1973 in U.S. Geological Survey Professional Paper 820, United States Mineral Resources. In 1973, many of these commodities were only of minor importance, and resource and geologic information was often very limited and incomplete. In addition, little was generally known about geoenvironmental issues related to their production and use.

We would like to thank our colleagues for their contributions to and cooperation in all phases of the preparation of this book. The descriptions of geology, the origin of mineral deposits, and geoenvironmental chemistry in each chapter necessarily involve some scientific jargon, but much of the discussion is cast in less-technical language. Our hope is that the information provided will be of use to scientists and non-scientists alike.

Klaus J. Schulz
John H. DeYoung, Jr.
Robert R. Seal II
Dwight C. Bradley

Contents

Foreword	iii
Preface	iv
Chapter A. Critical Mineral Resources of the United States—An Introduction By Klaus J. Schulz, John H. DeYoung, Jr., Dwight C. Bradley, and Robert R. Seal II	A1
Chapter B. Environmental Considerations Related to Mining of Nonfuel Minerals By Robert R. Seal II, Nadine M. Piatak, Bryn E. Kimball, and Jane M. Hammarstrom	B1
Chapter C. Antimony By Robert R. Seal II, Klaus J. Schulz, and John H. DeYoung, Jr. With contributions from David M. Sutphin, Lawrence J. Drew, James F. Carlin, Jr., and Byron R. Berger	C1
Chapter D. Barite (Barium) By Craig A. Johnson, Nadine M. Piatak, and M. Michael Miller	D1
Chapter E. Beryllium By Nora K. Foley, Brian W. Jaskula, Nadine M. Piatak, and Ruth Schulte	E1
Chapter F. Cobalt By John F. Slack, Bryn E. Kimball, and Kim B. Shedd	F1
Chapter G. Fluorine By Timothy S. Hayes, M. Michael Miller, Greta J. Orris, and Nadine M. Piatak	G1
Chapter H. Gallium By Nora K. Foley, Brian W. Jaskula, Bryn E. Kimball, and Ruth Schulte	H1
Chapter I. Germanium and Indium By W.C. Pat Shanks III, Bryn E. Kimball, Amy C. Tolcin, and David E. Guberman	I1
Chapter J. Graphite By Gilpin R. Robinson, Jr., Jane M. Hammarstrom, and Donald W. Olson	J1
Chapter K. Lithium By Dwight C. Bradley, Lisa L. Stillings, Brian W. Jaskula, LeeAnn Munk, and Andrew D. McCauley	K1
Chapter L. Manganese By William F. Cannon, Bryn E. Kimball, and Lisa A. Corathers	L1
Chapter M. Niobium and Tantalum By Klaus J. Schulz, Nadine M. Piatak, and John F. Papp	M1
Chapter N. Platinum-Group Elements By Michael L. Zientek, Patricia J. Loferski, Heather L. Parks, Ruth F. Schulte, and Robert R. Seal II	N1
Chapter O. Rare-Earth Elements By Bradley S. Van Gosen, Philip L. Verplanck, Robert R. Seal II, Keith R. Long, and Joseph Gambogi	O1
Chapter P. Rhenium David A. John, Robert R. Seal, II, and Désirée E. Polyak	P1
Chapter Q. Selenium By Lisa L. Stillings	Q1

Chapter R. Tellurium

By Richard J. Goldfarb, Byron R. Berger, Micheal W. George, and Robert R. Seal II R1

Chapter S. Tin

By Robert J. Kamilli, Bryn E. Kimball, and James F. Carlin, Jr. S1

Chapter T. Titanium

By Laurel G. Woodruff, George M. Bedinger, and Nadine M. Piatak T1

Chapter U. Vanadium

By Karen D. Kelley, Clinton T. Scott, Désirée E. Polyak, and Bryn E. Kimball U1

Chapter V. Zirconium and Hafnium

By James V. Jones III, Nadine M. Piatak, and George M. Bedinger V1

Figures

A1.	Diagram showing increases in the use of elements over two decades of computer chip technology development	A3
A2.	Diagram showing the mineral resource classification system used in this volume.....	A5
B1.	Graph showing population growth and the change in supporting land area from 3500 B.C. to 2100 A.D., with projections to 2050	B3
B2.	Graph showing dates associated with all the mine sites on the U.S. Environmental Protection Agency's National Priorities List	B10
C1.	World map showing the location of selected antimony deposits, mines, and major occurrences	C2
C2.	Pie chart showing end uses of antimony as a percentage of antimony consumption in the United States in 2012.....	C3
C3.	Graph showing world production, U.S. apparent consumption, and U.S. mine production of antimony from 1900 to 2012	C4
C4.	Pie charts showing percentages of contained antimony in U.S imports in 2008–11, by source country.....	C5
D1.	Graph showing barite world production, U.S. production, and U.S. consumption from 1950 to 2011.....	D2
D2.	Map showing locations of selected barite deposits and districts, color-coded by deposit type	D4
D3.	Pie chart showing the average annual tonnage of barite produced by country for the period 2007–11, in million metric tons.....	D7
E1.	Map showing locations of selected deposits of beryllium by the two major beryllium-bearing mineral types	E2
E2.	Photographs of the minerals bertrandite, which can contain up to 42 percent beryllium oxide, and industrial beryl, which can contain up to about 5 percent beryllium.....	E3
E3.	Photographs illustrating some of the many uses of beryllium	E4
E4.	Pie charts showing reported uses of beryllium consumed in the United States in 2011 for the two main classes of products—performance alloys, and beryllium and composites	E6
E5.	A generalized cross section showing the geologic setting of and some example deposits for the major types of beryllium resources associated with rare-metal magma systems.....	E12

E6.	Location map and simplified geologic map of the Hellroaring Creek prospect, which is located west of Kimberley, British Columbia, Canada.....	E13
E7.	Schematic geologic cross section showing the setting of volcanogenic beryllium deposits and related deposit types, geologic map of the Spor Mountain area in Utah, photograph of beryllium tuff at Spor Mountain, and photograph of nodule from the Spor Mountain tuff.....	E15
E8.	Graph showing general estimates of grade and tonnage for a variety of beryllium deposits, districts, and belts.....	E17
E9.	Graph showing estimated global production of beryllium, in metric tons, from 2000 to 2011.....	E18
F1.	Pie chart showing world cobalt consumption in 2011, by end use	F2
F2.	Graph showing world cobalt mine and refinery production and apparent consumption	F2
F3.	Graph showing world cobalt mine production from 1950 to 2011	F3
F4.	Pie chart showing world cobalt mine production in 2011, by country.....	F3
F5.	Pie chart showing world cobalt mine production in 2011, by deposit type	F10
F6.	Grade-tonnage plot for 214 cobalt deposits worldwide.....	F11
F7.	Map showing global distribution of major cobalt-bearing mineral deposits and selected smaller deposits that represent minor types	F12
F8.	Pie charts showing proportions of cobalt contained in mineral deposits worldwide, by deposit type	F13
G1.	Photograph of a fluorite specimen from the Number 1 (Minerva) Mine, Cave-in-Rock subdistrict, Illinois-Kentucky fluorspar district	G3
G2.	Graph showing the solubility of fluorite as a function of temperature for complex Na-Ca-Mg-Cl (sodium-calcium-magnesium-chloride) brines from ambient temperatures to 260° Celsius	G10
G3.	Chart showing eight minerals or mineral groups from which fluorine has been produced or may be produced in the future and a preliminary classification of hydrothermal fluorspar deposits by tectonic and magmatic association	G11
G4.	World map showing selected world fluorspar deposits according to their tectonic and magmatic class.....	G14
G5.	Map showing the locations of deposits in the Cantabrian salt-related carbonate-hosted mineral district in north-central Spain.....	G19
G6.	Plot of fluorite grade versus tonnage for fluorspar deposits related to strongly differentiated granites, for carbonatite-related fluorspar deposits, and for veins from all classes of fluorspar deposits	G24
G7.	Graph showing sources of U.S. fluorspar supply from 1970 to 2011	G29
H1.	Photograph of gallium metal with an inset showing its position on the periodic table of elements.....	H1
H2.	Photographs illustrating some current uses for gallium.....	H3
H3.	Graphs showing U.S. and world gallium production and consumption for 2007 to 2012.....	H4
H4.	World map showing the locations of selected mineral deposits, by type; gallium has been produced from these types of deposits.....	H5
H5.	Cross sections showing the general geologic environments for the types of mineral deposits with which gallium is most commonly associated and from which gallium is typically extracted	H7
H6.	Plot of the ratio of aluminum to gallium (Al:Ga, log scale) versus gallium content for volcanic rocks, hydrothermally altered rocks, and bauxite deposits	H12

H7.	Photographs showing samples of bauxite ore and sphalerite ore, which are the primary mineralogical sources of gallium	H14
I1.	Photograph of a concentrator photovoltaic solar power system	I3
I2.	Pie charts showing relative end uses of germanium and indium worldwide in 2012.....	I3
I3.	Photographs showing tin-doped indium oxide and examples of display screens that are coated with it.....	I4
I4.	Map and schematic cross section showing the geology of the Red Dog district in Alaska and the stratigraphy of selected deposits in the district.....	I7
I5.	Map showing the locations and geologic settings of selected volcanogenic massive sulfide, sedimentary exhalative, Mississippi Valley-type, and coal deposits and other types of deposits in southern China.....	I9
I6.	Map showing the location of Kipushi-type deposits (including the Kabwe deposits) and major Neoproterozoic orogenic belts and basins in the Precambrian tectonic framework of southern Africa	I10
I7.	Map showing indium-bearing tin-polymetallic ore deposits in Bolivia	I12
I8.	Graph showing worldwide production of germanium and indium from 1995 to 2012	I14
J1.	Diagram showing the arrangement of carbon atoms in crystalline graphite, which consists of stacks of parallel sheets of carbon atoms, with each sheet containing hexagonal arrays of carbon atoms.....	J6
J2.	Map showing locations of major graphite deposits and districts in the world, by commodity type.....	J14
J3.	Graph showing carbon grade and “ore” tonnage characteristics for some of the amorphous and crystalline graphite deposits	J16
J4.	Pie chart showing average estimated natural graphite production by country or region from 2006 to 2010, in thousand metric tons per year	J17
K1.	Graph showing lithium production, by deposit type, from 1900 through 2006	K1
K2.	Pie chart showing end uses of lithium as a percentage of worldwide lithium consumption for the year 2013	K2
K3.	Photographs illustrating some sources and uses of lithium	K3
K4.	World map showing lithium-cesium-tantalum pegmatites, by size, and lithium-enriched granites	K6
K5.	World map showing closed-basin lithium-brine, lithium-enriched oilfield brine, geothermal brine, lithium-clay, and lithium-zeolite deposits.....	K7
K6.	Histograms of the number of lithium-cesium-tantalum pegmatites formed per 50-million-year interval as a function of geologic time, of the age distribution of detrital zircon in river sand as a function of time, and of the age distribution of lithium resources in pegmatites	K9
K7.	Schematic cross section showing the concentric arrangement of lithium-cesium-tantalum pegmatites around a parental granite pluton	K10
K8.	Block diagram showing conceptual ore-deposit model for lithium brine.....	K11
K9.	Lithium grade-tonnage plots based on values from known deposits.....	K13
L1.	Bar chart showing world production of manganese ore from 2007 to 2011 compared with apparent consumption, and pie chart showing distribution of manganese ore production, by country, for the same period.....	L3
L2.	Pie charts showing the sources and the annual average amounts of U.S. imports of manganese ore, ferromanganese, and silicomanganese for the period 2008–11	L3
L3.	World map showing the location, relative size, and type of the major terrestrial manganese deposits listed in table L2 as well as subeconomic deposits in the United States	L7

L4.	Photographs of contrasting types of manganese ore	L8
L5.	Schematic diagram of the oceanic conditions necessary to form sedimentary manganese deposits that are not enriched in iron	L8
L6.	Photograph showing a dense carpet of ferromanganese nodules on the seabed off Johnston Island within the United States Exclusive Economic Zone near Hawaii.....	L10
L7.	Photograph showing ferromanganese crust on carbonate rock from the Blake Plateau off the southeastern coast of the United States.....	L11
L8.	Photograph of the Mamatwan open pit mine in South Africa	L13
L9.	Graphs showing the cumulative frequency of tonnages and grades of 39 marine sedimentary manganese deposits	L14
M1.	Photograph of the ATLAS detector in the Large Hadron Collider showing its eight superconducting barrel toroid magnets around the calorimeter.....	M3
M2.	Reported world consumption of niobium and tantalum, by material produced.....	M3
M3.	Criticality matrix for niobium, tantalum, and selected other mineral commodities.....	M4
M4.	Photographs showing centimeter-size pyrochlore crystals from Uganda and a tantalite crystal	M6
M5.	Map showing the locations of selected niobium and tantalum mines, deposits, and occurrences, by deposit type	M8
M6.	Log-log plots of tantalum and niobium deposit grades and tonnages, by deposit type	M9
M7.	Diagrams showing the subsurface geology of the Saint-Honoré carbonatite complex in southern Quebec, Canada, and a schematic north-south cross-section	M14
M8.	Schematic cross-section of the Lovozero alkaline intrusion, Kola Peninsula, Russia, showing the relation among the three intrusive phases and the niobium mineralization contained in eudialyte and loparite.....	M17
M9.	Schematic representation of regional lithium-cesium-tantalum rare-metal-bearing pegmatite zoning above a parental granite.....	M18
M10.	Schematic cross-section of a concentrically zoned lithium-cesium-tantalum rare-metal-bearing pegmatite	M18
M11.	Bar chart showing niobium resources and reserves in Brazil, Canada, and the United States, in thousand metric tons of Nb	M20
M12.	Bar chart showing global tantalum resources and reserves, in thousand metric tons of Ta.....	M21
M13.	Bar chart showing global production of primary niobium and tantalum from 2000 through 2011, in metric tons of contained metal produced.....	M23
M14.	Pie charts showing estimated annual average percentage of niobium production, and tantalum production, by country, for the period 2007–11	M23
N1.	Graphs showing platinum and palladium consumption, by category of use, from 2000 to 2012 for the world, North America, and China	N3
N2.	Photograph of gold mask with platinum highlights, from the period of La Tolita culture, Ecuador.....	N4
N3.	Map showing the locations of igneous intrusions and intrusive complexes that contain most of the world's platinum-group-element deposits, as well as the placer deposits that are mentioned in the text.....	N7
N4.	Schematic block diagram showing changes in the form of igneous intrusions with depth and the relative occurrence of conduit-type, contact-type, and reef-type magmatic ore deposits.....	N9

N5.	Map showing the geology of the Siberian flood basalt province in Russia	N10
N6.	Map showing the geology of the Noril'sk-Talnakh area and the location of nickel-copper-platinum-group-element deposits.....	N11
N7.	Maps showing nickel-copper-platinum-group-element deposits in the Talnakh area, Russia	N13
N8.	Photograph of copper-rich massive sulfide ore exposed in a stope in the Oktyabr'sk Mine in the Talnakh area, Russia	N14
N9.	Map showing the Rustenburg Layered Suite of the Bushveld Complex, South Africa, the surface trace of significant orebodies, and cross sections through the central area and northeastern limb	N15
N10.	Photograph of the UG2 Chromitite at the Karee Mine in the western part of the Bushveld Complex, South Africa	N16
N11.	Photograph of the base of the Merensky cyclic unit which contains the platinum-group-element-rich Merensky Reef	N16
N12.	Geologic map and cross sections of the Great Dyke, Zimbabwe	N17
N13.	Geologic map and cross section of the Stillwater Complex, Montana	N19
N14.	Photograph of the Stillwater Mine in south-central Montana, looking southeast.....	N20
N15.	Map showing the geology along the western margin of the Duluth Complex, Minnesota, with the surface projection of nickel-copper-platinum-group-element deposits and exploration targets.....	N21
N16.	Maps illustrating the distribution of platinum deposits in the Ural Mountains, Russia	N24
N17.	Geologic map and imagery of the Uralian-type Kondyor Massif in eastern Siberia, Russia.....	N25
N18.	Photograph and lithograph showing the morphology of platinum-iron-alloy nuggets derived from Uralian-type intrusions	N26
N19.	Maps illustrating platinum-group-element resources in southeastern Alaska	N27
N20.	Graph showing platinum-group-element production, by country, from 1960 to 2011.....	N28
N21.	Pie chart showing world platinum-group-element production, by country, from 1960 to 2011.....	N29
N22.	Plot showing the relation between tonnage and grade of remaining resources for conduit-type, reef-type, and other types of deposits enriched in platinum-group elements	N30
N23.	Graphs showing the percent of contained metal against percent of deposits for the world's platinum-group-element (PGE) and porphyry copper deposits and the top 30 percent of the world's PGE deposits	N31
N24.	Graph showing contained platinum-group element (PGE) and gold metal against the ratio of palladium to platinum for the major PGE deposits of the world	N32
N25.	Map and three-dimensional block diagram showing the Merensky Reef interpolated down to 2 kilometers in the southern area of the western limb of the Bushveld Complex, South Africa	N33
N26.	Graph illustrating the exposed area and stratigraphic thickness of cumulates in more than 200 intrusions from around the world	N34
N27.	Geologic map of the Amphitheater Mountains and south-central Alaska showing the location and names of mafic-ultramafic complexes that are part of the Nikolai large igneous province	N36

N28.	Graphs showing prices for platinum, palladium, rhodium, iridium, ruthenium, and osmium from 1880 to 2013.....	N44
01.	Graph showing world mine production of rare-earth oxides from 1960 to 2012.....	04
02.	Graph showing radii of the trivalent ions of the rare-earth elements, along with the radii of the cerium (Ce^{4+}) and europium (Eu^{2+}) ions.....	06
03.	Photograph of the Mountain Pass Mine, which was the only active producer of rare-earth elements in the United States in 2013.....	08
04.	Map showing the locations of active rare-earth element mines and ongoing advanced exploration projects.....	09
05.	Chondrite-normalized plot showing the rare-earth-element (REE) distribution in six different types of North American REE deposits.....	011
P1.	Photographs of rhenium and rhenium compounds.....	P2
P2.	Pie chart showing major end uses of primary rhenium as a percentage of total rhenium consumption in the world in 2012.....	P3
P3.	Map showing locations of major rhenium-bearing deposits, including porphyry copper-molybdenum-gold deposits.....	P5
P4.	Plot of rhenium grade versus deposit tonnage for major rhenium-bearing deposits in the world.....	P10
P5.	Cross sections illustrating rhenium occurrences in major deposit types from which rhenium is recovered or potentially recoverable.....	P11
P6.	Pie chart showing mine production of rhenium, by country, as a percentage of world mine production of rhenium in 2012.....	P18
Q1.	Graph showing relative abundance of the chemical elements in Earth's upper crust.....	Q2
Q2.	Graph showing end uses for selenium in the United States from 1975 to 2012.....	Q3
Q3.	Graph showing average annual prices of commercial-grade selenium from 1970 to 2010.....	Q5
Q4.	Map showing selenium concentrations (in parts per million) in coal samples, by region of the United States.....	Q16
Q5.	Maps showing locations of seleniferous sedimentary outcrops and deposits and plant samples with significant selenium content.....	Q17
Q6.	A predictive map of selenium source rocks associated with organic-rich depositional marine basins.....	Q21
Q7.	Maps showing selenium concentrations in soils of the conterminous United States.....	Q23
R1.	World map showing the locations of selected tellurium-enriched mineral occurrences discussed in the text, by type of deposit.....	R2
R2.	Pie chart showing major uses for tellurium in the world in 2010, by end use.....	R3
R3.	Phase diagram showing speciation calculations for tellurium in a hydrothermal fluid at 300 degrees Celsius, as a function of pH and oxygen fugacity.....	R4
R4.	Pie chart showing estimated tellurium refinery production, by region, as a percentage of world refinery production.....	R13
S1.	Pie chart showing end uses of tin as a percentage of total consumption in the United States in 2014.....	S4
S2.	Graph showing the average annual prices of tin metal from 1970 to 2010.....	S5
S3.	Ball-and-stick model of part of the crystal structure of cassiterite.....	S6
S4.	Photograph of cassiterite crystals.....	S6

S5.	Photograph of wood tin cassiterite	S6
S6.	Schematic vertical section across a typical hydrothermal mineralized granite cupola showing salient features of a shallow granite-related tin-mineralized system	S7
S7.	Map showing locations of major tin deposits and districts in the world, by deposit type	S10
S8.	Graph showing grades and resource tonnages of major tin deposits in the world, by deposit type	S11
S9.	Pie chart showing world tin reserves, by country, as a percentage of the world total of 4.7 million metric tons, in 2016	S12
S10.	Pie chart showing tonnage and distribution of estimated world mine production of tin, by country, in 2015	S12
S11.	Map of Alaska showing the locations of selected tin deposits	S15
T1.	Chart showing common titanium-bearing oxide minerals and common titanium-bearing silicate minerals with their approximate titanium content	T5
T2.	Reflected-light photographs showing lamellae of hematite in ilmenite in hemo-ilmenite from the magmatic Lac Tio hemo-ilmenite deposit, and titaniferous magnetite and ilmenite from the magmatic La Blache iron-titanium-oxide deposit	T5
T3.	Map showing worldwide distribution of titanium deposits	T7
T4.	Graph showing comparison of approximate titanium dioxide content in titanium deposits of different deposit types	T8
T5.	Plot of titanium grade and tonnage for some igneous, metamorphic, and sedimentary deposits	T10
T6.	Pie charts showing estimated 2012 world mine production, by country, of ilmenite and rutile, and global reserves of ilmenite and rutile, in metric tons	T11
U1.	World map showing global distribution of major vanadium deposits, by deposit type	U3
U2.	Pie chart showing the world's leading vanadium-producing countries in 2012 by percentage of world production	U9
U3.	Graph showing major end uses of vanadium in the United States from 1970 to 2011	U9
U4.	Photographs of example sources and uses of vanadium	U12
U5.	Grade-tonnage diagram of vanadium deposits for which data were available	U19
V1.	Photographs of example sources and uses of zirconium and hafnium	V3
V2.	Graphs showing global zirconium production and U.S. trade information for zirconium ores and concentrates	V4
V3.	World map showing selected zirconium and hafnium deposits and regions with modern coastal placer systems	V8
V4.	Diagrams showing examples of coastal depositional systems with an emphasis on barrier island location, morphology, and depositional environments	V10
V5.	Diagrams showing influences on and locations of placer formation in coastal environments	V11

Tables

A1.	Crustal abundances of mineral commodities (elements) included in this volume	A6
B1.	Summary of selected Federal laws relevant to mine permitting	B4
B2.	Historical summary of mine sites placed on the U.S. Environmental Protection Agency's National Priorities List	B8
B3.	Selected consortia devoted to identifying and implementing environmental best practices associated with mining	B11
C1.	Selected antimony minerals	C7
C2.	Estimated world production and reserves of antimony in 2013	C9
C3.	Potential additional sources of antimony ore and concentrate, by country	C10
E1.	Selected properties of beryllium, which is a Group 2 alkaline earth metal	E5
E2.	Selected beryllium minerals	E8
E3.	Global and domestic types of magmatic-related beryllium resources	E10
E4.	Grade and tonnage data for selected beryllium deposits	E22
F1.	Location and grade-tonnage data for significant cobalt deposits of the world	F33
F2.	Cobalt concentrations in rocks, soils, waters, and air	F6
G1.	Fluorine concentrations in various types of rocks	G5
G2.	Concentrations of fluorine and other elements in waters	G6
G3.	Selected examples of the chemistry and mineralogy of mine waste generated at fluorspar mines	G34
G1–1.	Selected fluorspar districts, deposits, and prospects of the world	G54
H1.	Selected properties of gallium, a Group 13 post-transition metal	H8
H2.	Concentrations of gallium in rocks, ore, coal, soils, and natural waters	H9
H3.	Gallium-bearing minerals—formulas, content, and occurrence	H13
H4.	Significant global and domestic deposit types from which gallium is obtained or is potentially extractable	H16
I1.	Classification of deposits that host germanium and indium resources	I6
I2.	Average estimated annual refinery production of germanium and indium, by area, or 2011 and 2012	I14
I3.	Germanium concentrations in rocks, soils, and waters	I16
I4.	Indium concentrations in rocks, soils, waters, and air	I17
J1.	Characteristics of graphite commodities, deposits, and uses, by commodity type	J2
J2.	Physical properties of graphite	J3
J3.	Selected information for graphite deposits and districts	J9
J4.	Estimates of world graphite resources, by country, commodity type, and resource category, in thousand metric tons of recoverable graphite	J18
K1.	Commercially and (or) scientifically important lithium-bearing minerals	K5
K2.	Lithium concentrations in soils developed on various types of bedrock	K15
L1.	Estimated world manganese ore reserves in 2012, in thousand metric tons of contained manganese	L3

L2.	Total resources estimated for major land-based manganese deposits of the world	L13
L3.	Grade, tonnage, and quantity of contained manganese for eight manganese deposits and districts in the United States.....	L16
L4.	Background and above-background concentrations of manganese in rocks, soil, water, and air	L19
M1.	Selected properties of niobium and tantalum	M2
M2.	Selected niobium and tantalum oxide minerals and their end-member Nb_2O_5 and Ta_2O_5 contents or compositional range.....	M5
M3.	Major types of niobium and tantalum deposits, with key characteristics and examples	M7
M4.	Locations of selected niobium-tantalum deposits, with grade and tonnage	M10
N1.	Chemical formulas for selected platinum-group minerals as well as other common rock-forming minerals mentioned in this report.....	N6
N2.	Examples of rocks and ores with anomalous platinum-group-element concentrations that are not associated with magmatic deposits, by deposit types	N70
N3.	Areas with significant placer platinum production, and estimates of cumulative production and grades.....	N23
N4.	Identified platinum-group-element and gold resources, summarized by deposit type and location	N29
N5.	Igneous intrusions and intrusive complexes that contain more than 97 percent of the world's identified platinum-group-element (PGE) and gold resources, in order of total contained PGEs	N74
N6.	Areal extent and stratigraphic thickness of layered intrusions with reef-type platinum-group-element deposits and some examples of large intrusions with no known deposits, in order of areal extent.....	N75
N7.	Platinum-group-element concentrations in samples of upper crust, loess, river sediment, and marine pelagic sediment.....	N38
N8.	Trace element geochemistry of waters from selected conduit-type, contact-type, and reef-type deposits.....	N77
N9.	Acid-base accounting for selected reef-type, contact-type, and conduit-type deposits.	N79
N10.	Grade and tonnage of mineralized rock remaining in platinum-group-element-bearing mineral deposits.....	N80
O1.	List of the rare-earth elements found in natural deposits—the “lanthanides” plus yttrium	O2

02.	List of selected rare-earth-element-bearing and yttrium-bearing ore minerals	010
03.	Active rare-earth mines by deposit type	012
04.	Advanced rare-earth-element (REE) exploration projects and the reported estimates of their REE resources by deposit type.....	014
P1.	Summary of rhenium, copper, and molybdenum grades, deposit tonnage, and amount of contained rhenium in the rhenium-bearing deposits shown in figure P3.....	P6
P2.	Rhenium data for porphyry copper and porphyry molybdenum deposits.....	P38
P3.	Concentrations of rhenium in water, sediments, soils, biota, and upper continental crust.....	P20
Q1.	Selenium minerals recognized by the International Mineralogical Association.....	Q42
Q2.	A summary of selenium concentrations in various selenides and sulfides from deposits around the world	Q47
Q3.	Selenium concentration in sulfide minerals and other phases, in various deposit types	Q9
Q4.	Selenium concentrations in copper-nickel ores in the Sudbury basin, Ontario, Canada	Q11
Q5.	Selenium concentrations in selected Earth and lunar materials	Q14
Q6.	Estimated world selenium reserves in 2014, in metric tons.....	Q20
Q7.	National Institutes of Health recommended dietary reference intakes for selenium.....	Q30
R1.	Tellurium-bearing minerals, many of which are mentioned in this chapter.....	R5
S1.	List of selected tin-bearing minerals.....	S3
S2.	Tin deposits with more than 1,000 metric tons of contained tin, including location, grade, and deposit tonnage.....	S32
S3.	Tin reserves of the world in 2016, in metric tons of contained tin	S11
S4.	Tin concentrations in rocks, soils, water, and air	S17
T1.	Classification of selected titanium mineral deposits based on their geologic setting and the processes through which they were formed	T3
T2.	Titanium resources of the United States	T13
T3.	Titanium mineral resources of the world (excluding the United States) for ilmenite (including titanomagnetite and leucoxene) and rutile (including anatase and brookite)	T14
U1.	Location and grade-tonnage of vanadium mineral deposits	U4
U2.	Mineralogy of standard vanadium-bearing minerals in different deposit types	U11
U3.	Concentrations of vanadium in rock, soils, water, and air.....	U23

Conversion Factors

International System of Units to Inch/Pound

Multiply	By	To obtain
Length		
angstrom (Å) (0.1 nanometer)	0.003937	microinch
angstrom (Å) (0.1 nanometer)	0.000003937	mil
micrometer (μm) [or micron]	0.03937	mil
millimeter (mm)	0.03937	inch (in.)
centimeter (cm)	0.3937	inch (in.)
meter (m)	3.281	foot (ft)
meter (m)	1.094	yard (yd)
kilometer (km)	0.6214	mile (mi)
Area		
hectare (ha)	2.471	acre
square kilometer (km ²)	247.1	acre
square meter (m ²)	10.76	square foot (ft ²)
square centimeter (cm ²)	0.1550	square inch (in ²)
square kilometer (km ²)	0.3861	square mile (mi ²)
Volume		
milliliter (mL)	0.03381	ounce, fluid (fl. oz)
liter (L)	33.81402	ounce, fluid (fl. oz)
liter (L)	1.057	quart (qt)
liter (L)	0.2642	gallon (gal)
cubic meter (m ³)	264.2	gallon (gal)
cubic centimeter (cm ³)	0.06102	cubic inch (in ³)
cubic meter (m ³)	1.308	cubic yard (yd ³)
cubic kilometer (km ³)	0.2399	cubic mile (mi ³)
Mass		
microgram (μg)	0.0000003527	ounce, avoirdupois (oz)
milligram (mg)	0.00003527	ounce, avoirdupois (oz)
gram (g)	0.03527	ounce, avoirdupois (oz)
gram (g)	0.03215075	ounce, troy
kilogram (kg)	32.15075	ounce, troy
kilogram (kg)	2.205	pound avoirdupois (lb)
ton, metric (t)	1.102	ton, short [2,000 lb]
ton, metric (t)	0.9842	ton, long [2,240 lb]
Deposit grade		
gram per metric ton (g/t)	0.0291667	ounce per short ton (2,000 lb) (oz/T)
Pressure		
megapascal (MPa)	10	bar
gigapascal (GPa)	10,000	bar
Density		
gram per cubic centimeter (g/cm ³)	62.4220	pound per cubic foot (lb/ft ³)
milligram per cubic meter (mg/m ³)	0.0000006243	pound per cubic foot (lb/ft ³)
Energy		
joule (J)	0.0000002	kilowatthour (kWh)
joule (J)	6.241×10^{18}	electronvolt (eV)
joule (J)	0.2388	calorie (cal)
kilojoule (kJ)	0.0002388	kilocalorie (kcal)

Conversion Factors—Continued

International System of Units to Inch/Pound

Multiply	By	To obtain
Radioactivity		
becquerel (Bq)	0.00002703	microcurie (μCi)
kilobecquerel (kBq)	0.02703	microcurie (μCi)
Electrical resistivity		
ohm meter ($\Omega\text{-m}$)	39.37	ohm inch ($\Omega\text{-in.}$)
ohm-centimeter ($\Omega\text{-cm}$)	0.3937	ohm inch ($\Omega\text{-in.}$)
Thermal conductivity		
watt per centimeter per degree Celsius ($\text{watt/cm } ^\circ\text{C}$)	693.1798	International British thermal unit inch per hour per square foot per degree Fahrenheit ($\text{Btu in/h ft}^2 ^\circ\text{F}$)
watt per meter kelvin (W/m-K)	6.9318	International British thermal unit inch per hour per square foot per degree Fahrenheit ($\text{Btu in/h ft}^2 ^\circ\text{F}$)

Inch/Pound to International System of Units

Length		
mil	25.4	micrometer (μm) [or micron]
inch (in.)	2.54	centimeter (cm)
inch (in.)	25.4	millimeter (mm)
foot (ft)	0.3048	meter (m)
mile (mi)	1.609	kilometer (km)
Volume		
ounce, fluid (fl. oz)	29.57	milliliter (mL)
ounce, fluid (fl. oz)	0.02957	liter (L)
Mass		
ounce, avoirdupois (oz)	28,350,000	microgram
ounce, avoirdupois (oz)	28,350	milligram
ounce, avoirdupois (oz)	28.35	gram (g)
ounce, troy	31.10 348	gram (g)
ounce, troy	0.03110348	kilogram (kg)
pound, avoirdupois (lb)	0.4536	kilogram (kg)
ton, short (2,000 lb)	0.9072	ton, metric (t)
ton, long (2,240 lb)	1.016	ton, metric (t)
Deposit grade		
ounce per short ton (2,000 lb) (oz/T)	34.285714	gram per metric ton (g/t)
Energy		
kilowatthour (kWh)	3,600,000	joule (J)
electronvolt (eV)	1.602×10^{-19}	joule (J)
Radioactivity		
microcurie (μCi)	37,000	becquerel (Bq)
microcurie (μCi)	37	kilobecquerel (kBq)

Temperature in degrees Celsius ($^\circ\text{C}$) may be converted to degrees Fahrenheit ($^\circ\text{F}$) as follows:

$$^\circ\text{F} = (1.8 \times ^\circ\text{C}) + 32$$

Temperature in degrees Celsius ($^\circ\text{C}$) may be converted to Kelvin (K) as follows:

$$\text{K} = ^\circ\text{C} + 273.15$$

Temperature in degrees Fahrenheit ($^\circ\text{F}$) may be converted to degrees Celsius ($^\circ\text{C}$) as follows:

$$^\circ\text{C} = (^\circ\text{F} - 32) / 1.8$$

Datum

Unless otherwise stated, vertical and horizontal coordinate information is referenced to the World Geodetic System of 1984 (WGS 84). Altitude, as used in this report, refers to distance above the vertical datum.

Supplemental Information

Specific conductance is given in microsiemens per centimeter at 25 degrees Celsius ($\mu\text{S}/\text{cm}$ at 25 °C).

Concentrations of chemical constituents in soils and (or) sediment are given in milligrams per kilogram (mg/kg), parts per million (ppm), or parts per billion (ppb).

Concentrations of chemical constituents in water are given in milligrams per liter (mg/L), micrograms per liter ($\mu\text{g}/\text{L}$), nanograms per liter (ng/L), nanomoles per kilogram (nmol/kg), parts per million (ppm), parts per billion (ppb), or parts per trillion (ppt).

Concentrations of suspended particulates in water are given in micrograms per gram ($\mu\text{g}/\text{g}$), milligrams per kilogram (mg/kg), or femtograms per gram (fg/g).

Concentrations of chemicals in air are given in units of the mass of the chemical (milligrams, micrograms, nanograms, or picograms) per volume of air (cubic meter or cubic feet).

Activities for radioactive constituents in air are given in microcuries per milliliter ($\mu\text{Ci}/\text{mL}$).

Deposit grades are commonly given in percent, grams per metric ton (g/t)—which is equivalent to parts per million (ppm)—or troy ounces per short ton (oz/T).

Geologic ages are expressed in mega-annum (Ma, million years before present, or 10^6 years ago) or giga-annum (Ga, billion years before present, or 10^9 years ago).

Concentration unit	Equals
milligram per kilogram (mg/kg)	part per million
microgram per gram ($\mu\text{g}/\text{g}$)	part per million
microgram per kilogram ($\mu\text{g}/\text{kg}$)	part per billion (10^9)

Equivalencies

part per million (ppm): 1 ppm = 1,000 ppb = 1,000,000 ppt = 0.0001 percent

part per billion (ppb): 0.001 ppm = 1 ppb = 1,000 ppt = 0.0000001 percent

part per trillion (ppt): 0.000001 ppm = 0.001 ppb = 1 ppt = 0.0000000001 percent

Metric system prefixes

tera- (T-)	10^{12}	1 trillion
giga- (G-)	10^9	1 billion
mega- (M-)	10^6	1 million
kilo- (k-)	10^3	1 thousand
hecto- (h-)	10^2	1 hundred
deka- (da-)	10	1 ten
deci- (d-)	10^{-1}	1 tenth
centi- (c-)	10^{-2}	1 hundredth
milli- (m-)	10^{-3}	1 thousandth
micro- (μ -)	10^{-6}	1 millionth
nano- (n-)	10^{-9}	1 billionth
pico- (p-)	10^{-12}	1 trillionth
femto- (f-)	10^{-15}	1 quadrillionth
atto- (a-)	10^{-18}	1 quintillionth

Abbreviations and Symbols

3TG	tantalum, tin, tungsten, and (or) gold
Å	angstrom
AC	alternating current
ADTI	Acid Drainage Technology Initiative
AFRG	alkali-feldspar rhyolite-granite
Ag ₂ S	acanthite
Ag ₂ Se	naumannite
Ag ₄ SeS	aguilarite
Ag ₈ GeS ₆	argyrodite
Ag ₈ SnS ₆	canfieldite
AIDS	acquired immunodeficiency syndrome
AlF ₃	aluminum fluoride
Al(OH) ₃	gibbsite
AlMnO ₂ (OH) ₂	lithiophorite
Al ₂ O ₃	aluminum oxide (alumina)
Al ₂ SiO ₅	kyanite
AMD	acid mine drainage
AMT	audio magnetotelluric
API	American Petroleum Institute
APS	American Physical Society
ATPC	Association of Tin Producing Countries
ATSDR	Agency for Toxic Substances and Disease Registry
AuAg(S,Se)	petrovskaitite
BaCO ₃	barium carbonate (witherite)
BaMn ₉ O ₁₆ (OH) ₄	romanechite
BaSi ₂ O ₅	sanbornite
BaSO ₄	barium sulfate (barite)
BCMA	beryllium-copper master alloy
BeAl ₂ O ₄	chrysoberyl
BeAlSiO ₄ (OH)	euclase
BeCl ₂	beryllium chloride
BeO	beryllium oxide
Be ₂ SiO ₄	phenakite
BeSO ₄	beryllium sulfate
Bi ₂ Se ₃	guanajuatite
Bi ₂ Te ₂ S	tetradymite
Bq/kg	becquerel per kilogram
°C	degree Celsius
ca.	circa
CaCO ₃	calcium carbonate (calcite)

CaF_2	calcium fluoride (fluorite, also known as fluorspar)
$(\text{CaMg})(\text{CO}_3)_2$	dolomite
$\text{Ca}(\text{Mg}, \text{Fe}^{2+}, \text{Mn})(\text{CO}_3)_2$	ankerite
$(\text{Ca}, \text{Na})_2\text{Nb}_2\text{O}_6\text{F}$	pyrochlore
CaO	calcium oxide
CaSO_4	anhydrite
$\text{CaSO}_4 \cdot 2\text{H}_2\text{O}$	gypsum
CaTiO_3	perovskite ???
CaTiSiO_4	titanite
CaTiSiO_5	titanite or sphene
CBMM	Companhia Brasileira de Metalurgia e Mineração
CCD	carbonate compensation depth
CCZ	Clarion-Clipperton zone
CeO	cerium oxide
CERCLA	Comprehensive Environmental Response, Compensation, and Liability Act
CH_4	methane
CIGS	copper-indium-gallium-(di)selenide
cm	centimeter
cm^3	cubic centimeter
CO_2	carbon dioxide
$\text{Co}_3(\text{AsO}_4)_2 \cdot 8\text{H}_2\text{O}$	erythrite
Co_3S_4	linnaeite
CoAsS	cobaltite
Congo (Kinshasa)	Democratic Republic of the Congo
$\text{CoO}(\text{OH})$	heterogenite
CoSe_2	trogtalite
CPV	concentrator photovoltaic
CRD	carbonate replacement deposit
$\text{Cu}(\text{Co}, \text{Ni})_2\text{S}_4$	carrollite
$(\text{Cu}, \text{Fe})_{12}\text{As}_4\text{S}_{13}$	tennantite
$\text{Cu}_{13}\text{Fe}_2\text{Ge}_2\text{S}_{16}$	germanite
$\text{Cu}_9(\text{Fe}, \text{Ni})_8\text{S}_{16}$	talnakhite
CuFeS_2	chalcopyrite
Cu_5FeS_4	bornite
$\text{Cu}_9\text{Fe}_9\text{S}_{16}$	mooihoekite
$\text{Cu}_2\text{FeSnS}_4$	stannite
$(\text{Cu}, \text{Ni}, \text{Co}, \text{Fe})(\text{S}, \text{Se})_2$	selenium-rich villamaninite
CuS	covellite
Cu_2S	chalcocite
Cu_9S_5	digenite
Cu_2Se	berzelianite
CuSe_2	krutaite

Cu_3Se_2	umangite
$(\text{Cu,Zn})_{11}(\text{Ge,As})_2\text{Fe}_4\text{S}_{16}$	renierite
DC	direct current
DOD	U.S. Department of Defense
DRC	Democratic Republic of the Congo (Congo [Kinshasa])
EA	environmental assessment
EC_{50}	effective concentration 50 (concentration that results in 50 percent exhibiting decreased functionality)
EEZ	Exclusive Economic Zone
Eh	oxidation potential
EIS	environmental impact statement
EMPA	electron microprobe analysis
EPA	U.S. Environmental Protection Agency
FCC	fluid catalytic cracking
$\text{FeAsO}_4 \cdot 2\text{H}_2\text{O}$	scorodite
$\text{Fe}^{2+}\text{CO}_3$	siderite
$(\text{Fe,Mn})(\text{Ta,Nb})_2\text{O}_6$	tantalite
$(\text{Fe,Mn})\text{WO}_4$	wolframite
FeNb	ferroniobium
$(\text{Fe,Ni,Co})_9\text{S}_8$	pentlandite ???
Fe_2O_3	iron oxide (hematite)
$\text{Fe}^{3+}\text{O}(\text{OH})$	goethite ???
Fe_3O_4	magnetite
$\text{FeO}(\text{OH}) \cdot n\text{H}_2\text{O}$	limonite
FeOOH	goethite
FeS_2	pyrite
Fe_{1-x}S	pyrrhotite
FeSe_2	ferroselite
FeTiO_3	ilmenite
$\text{Fe}_2\text{Ti}_3\text{O}_9$	pseudorutile
Fe_2TiO_4	ulvöspinel
Fe_2TiO_5	pseudobrookite
FeV	ferrovanadium
FL–T	Fish Lake and Tangle
FONSI	finding of no significant impact
ft	foot
g	gram
$\text{g CO}_2\text{-equiv/kWh}$	gram of CO_2 equivalent per kilowatthour
g/cm^3	gram per cubic centimeter
g/d	gram per day
g/L	gram per liter
g/t	gram per metric ton

Ga	giga-annum (billion years before present, or 10 ⁹ years ago)
GaAs	gallium arsenide
GaN	gallium nitride
GARD	Global Acid Rock Drainage
GeCl ₄	germanium tetrachloride
GeH ₄	germane
GeO ₂	germanium dioxide
GWh	gigawatt-hour
H ₂	hydrogen gas
H ₂ O	water
H ₂ S	hydrogen sulfide
H ₂ Se	hydrogen selenide
HCl	hydrogen chloride
HDC	Hicks Dome Corp.
HF	hydrofluoric acid
HFO	hydrous ferric oxide
HFSE	high-field-strength element
(Hf,Zr)SiO ₄	hafnon
HgS	cinnabar
HgSe	tiemannite
HIV	human immunodeficiency virus
HMIS	Hazardous Materials Identification System
HREE	heavy rare-earth element
HSLA	high-strength, low-alloy
IARC	International Agency for Research on Cancer
ICP–MS	inductively coupled plasma-mass spectrometry
IED	improvised explosive device
IMA	International Mineralogical Association
In(NO ₃) ₃	indium nitrate
INAP	International Network for Acid Prevention
IOCG	iron oxide-copper-gold
IREL	Indian Rare Earths Ltd.
ISA	International Seabed Authority
ISMI	International Strategic Minerals Inventory
ITO	indium-tin oxide
JORC	Joint Ore Reserves Committee (Australia)
K(Mn ⁴⁺ ,Mn ²⁺) ₈ O ₁₆	cryptomelane
Kb ₂ Sb ₂ (C ₄ H ₂ O ₆) ₂	antimony/tartrate
kBq/kg	kilobecquerel per kilogram
KFe ^{III} ₃ (OH) ₆ (SO ₄) ₂	jarosite
kg	kilogram
kg CaCO ₃ /t	kilogram of calcium carbonate per metric ton

kg/cm ²	kilogram per square centimeter
kg/m ³	kilogram per cubic meter
kg/t	kilogram per metric ton
km	kilometer
km ²	square kilometer
km ³	cubic kilometer
KMML	Kerala Minerals and Metals Ltd.
KUCC	Kennecott Utah Copper Corp.
lb	pound
LC ₅₀	lethal concentration 50 (concentration that leads to 50 percent mortality)
LCT	lithium-cesium-tantalum
LED	light-emitting diode
Li ₂ CO ₃	lithium carbonate (zabuyelite)
Li ₂ O	lithium oxide
LIP	large igneous province
LOEL	lowest observable effect limit
log f O ₂	log of oxygen fugacity
LREE	light rare-earth element
m	meter
M	molarity
m.y.	million years
m ³	cubic meter
Ma	mega-annum (million years before present, or 10 ⁶ years ago)
MC–ICP–MS	multiple collector-inductively coupled plasma-mass spectrometry
MDEQ	Michigan Department of Environmental Quality
MEND	Mine Environment Neutral Drainage
mg	milligram
mg Al/kg	milligram of aluminum per kilogram
mg/d	milligram per day
mg/kg	milligram per kilogram
mg/L	milligram per liter
mg/m ³	milligram per cubic meter
(Mg,Fe) ₃ (Si,Al) ₄ O ₁₀ (OH) ₂ (Mg,Fe) ₃ (OH) ₆	chlorite
MgO	magnesium oxide
Mkg/yr	million kilograms per year
mm	millimeter
Mn ²⁺ Mn ³⁺ ₆ (SiO ₄)O ₈	braunite
MnCO ₃	rhodochrosite
MnO (OH)	manganite
MnO ₂	pyrolusite
MOFCOM	Ministry of Commerce (China)

monoclinic $\text{Na}_3(\text{AlF}_6)$	cryolite
MoS_2	molybdenite
MoSe_2	molybdenum (di)selenide
MRDS	Mineral Resources Data System
MRI	magnetic resonance imaging
MRS	Materials Research Society
MSS	monosulfide solution
MTR	Maderia-Tore Rise
MVT	Mississippi Valley-type
$(\text{Na,Ca,Ce})_2(\text{Nb,Ti,Ta})_2(\text{O,OH,F})$	pyrochlore group ???
$\text{Na}_{15}\text{Ca}_6\text{Fe}_3\text{Zr}_3\text{Si}_{26}\text{O}_{73}(\text{OH})_4\text{Cl}_2$	eudialyte
$(\text{Na,Ca,K,Ba,Sr})_{0.3-0.7}(\text{Mn,Mg,Al})_6\text{O}_{12}\cdot 3.2-4.5\text{H}_2\text{O}$	todorokite
NaCl	sodium chloride
NaHCO_3	sodium bicarbonate
Na_2O	sodium oxide
Nb_2O_5	niobium pentoxide
NEPA	National Environmental Policy Act
NFPA	National Fire Protection Association
ng/L	nanogram per liter
ng/m ³	nanogram per cubic meter
$(\text{NH}_4)^2\text{BeF}_4$	ammonium fluoroberyllate ???
NH_4ReO_4	ammonium perrhenate
NI	National Instrument
$(\text{Ni,Co,Cu})\text{Se}_2$	penroseite (blockite)
$(\text{Ni,Co})_{2-x}\text{Mn}(\text{O,OH})_4\cdot n\text{H}_2\text{O}$	asbolane
$(\text{Ni,Co})_3\text{S}_2$	heazlewoodite
$\text{Ni}(\text{S,Se})_2$	selenium-rich vaesite
$\text{Ni}(\text{S})_2$	vaesite
NiMH	nickel-metal-hydride
NIOSH	National Institute for Occupational Safety and Health
NMRI	nuclear magnetic resonance instruments
NPL	National Priorities List (Superfund)
NREL	National Renewable Energy Laboratory
NTP	National Toxicology Program
OPEC	Organization of the Petroleum Exporting Countries
org-Se(-II)	organo-selenide
OSHA	Occupational Safety and Health Administration
P_2O_5	phosphorus pentoxide ???
PbMoO_4	wulfenite
$\text{Pb}_3\text{Sn}_3\text{Sb}_2\text{S}_{14}$	cylindrite
$\text{Pb}_5\text{Sn}_3\text{Sb}_2\text{S}_{14}$	franckeite

PbS	lead sulfide (galena)
PbSe	clausthalite
PEM	proton exchange membrane
PET	polyethylene terephthalate
pg/L	picogram per liter
pg/m ³	picogram per cubic meter
PGE	platinum-group element
PGM	platinum-group metal
pm	picometer
ppb	part per billion
ppm	part per million
ppt	part per trillion
QSP	quartz-sericite-pyrite
RDA	recommended daily allowance
Re ⁰	native rhenium
Re ₂ O ₇	rhenium heptoxide
REE	rare-earth element
ReMoCu ₂ PbS ₆	copper-rhenium sulfide ???
REO	rare-earth oxide
ReO ₂	rhenium dioxide
ReO ₃	rhenium trioxide
ReS ₂	rheniite
RF	radio-frequency
SAF	submerged-arc furnace
SAMREC	South African Code for Reporting Exploration Results
Sb ₂ O ₃	antimony trioxide (senarmontite)
Sb ₂ S ₂ O	kermesite
Sb ₂ S ₃	stibnite
Sb ₃ O ₆ (OH)	stibiconite
SbCl ₃	antimony trichloride
Se	selenium
Se(-II)	selenide
Se(IV) or SeO ₃ ²⁻	selenite
Se(VI) or SeO ₄ ²⁻	selenate
Se ⁰	native selenium
SEC	U.S. Securities and Exchange Commission
SEDEX	sedimentary exhalative
SeO ₂	downeyite
SeO _{2(g)}	selenium dioxide
SG	specific gravity
SHRIMP	sensitive high-resolution ion microprobe
SiO ₂	silicon dioxide (quartz, amorphous silica)

SnCl_2	tin chloride
SnO_2	cassiterite
$\text{SO}_{2(\text{g})}$	sulfur dioxide
SO_4^{2-}	sulfate
^{86}Sr	isotope 86 for strontium
^{87}Sr	isotope 87 for strontium
SSV	sandstone-hosted vanadium
SX–EW	solvent extraction-electrowinning
Ta_2O_5	tantalum pentoxide
TBT	tributyltin
TBTCI	tributyltin chloride
TBTO	bis(tri-n-butyltin) oxide
$\text{Te}(\text{II})$	telluride
$\text{Te}(\text{IV})$	tellurite
$\text{Te}(\text{VI})$	tellurate
ThO_2	thorium dioxide
TiO_2	titanium dioxide (rutile, anatase, brookite)
TPT	triphenyltin
TRE	Tantalus Rare Earths
TREO	total rare-earth oxide
TWA	time-weighted average
UO_2	uranium dioxide
USGS	U.S. Geological Survey
UST	unidirectional solidification texture
V_2O_5	vanadium pentoxide
VLF	very low frequency
VMS	volcanogenic massive sulfide
VRB	vanadium redox-flow battery
VTM	vanadiferous titanomagnetite
WGS 84	World Geodetic System of 1984
WHO	World Health Organization
WO_3	tungsten trioxide
wt. %	weight percent
Y_2O_3	yttrium oxide (yttria)
ZnS	zinc sulfide (sphalerite)
ZnSe	stilleite
ZrO_2	zirconium dioxide (zirconia, baddeleyite)
ZrSiO_4	zircon
$\alpha\text{-AlO}(\text{OH})$	diaspore
$\alpha\text{-tin}$	alpha-tin (also known as gray tin)
$\beta\text{-tin}$	beta-tin (also known as white tin)
$\delta\text{-MnO}_2$	delta-manganese dioxide

γ -AlO(OH)	boehmite
$\mu\text{Ci/mL}$	microcurie per milliliter
$\mu\text{g Al/L}$	microgram of aluminum per liter
$\mu\text{g Mn/L}$	microgram of manganese per liter
$\mu\text{g Mn/m}^3$	microgram of manganese per cubic meter
$\mu\text{g/d}$	microgram per day
$\mu\text{g/g}$	microgram per gram
$\mu\text{g/kg}$	microgram per kilogram
$\mu\text{g/L}$	microgram per liter
$\mu\text{g/m}^3$	microgram per cubic meter
μm	micrometer

If no more rows are deleted, reduce space after a bit so can delete pages xxix and xxx

Prepared by the USGS Science Publishing Network
Reston Publishing Service Center

Edited by J.C. Ishee and Stokely J. Klasovsky

Illustrations and layout by Caryl J. Wipperfurth

For more information concerning this report,
please contact:

Mineral Resources Program Coordinator

U.S. Geological Survey

913 National Center

Reston, VA 20192

Telephone: 703-648-6100

Fax: 703-648-6057

Email: minerals@usgs.gov

Home page: <http://minerals.usgs.gov>



ISSN 1044-9612 (print)
ISSN 2330-7102 (online)
<http://dx.doi.org/10.3133/pp1802>

